Supplementary information for:

CRISPRi screen identifies FprB as a synergistic target for gallium therapy in *Pseudomonas aeruginosa*

Yu Zhang[1], Tingting Zhang[1,2], Xue Xiao[1], Yejun Wang[1], Adam Kawalek[3], Jinzhao Ou[1,2], Anmin Ren[4], Wenhao Sun[1], Vincent de Bakker[5], Yujie Liu[6], Yuelong Li[4], Liang Yang[4], Liang Ye[1], Ning Jia[4], Jan-Willem Veening[5], Xue Liu[1,2*]

[1]Guangdong Provincial Key Laboratory of Regional Immunity and Diseases, Department of Pathogen Biology, Shenzhen University Medical School, Shenzhen 518055, Guangdong, China.

[2]Guangdong Key Laboratory for Biomedical Measurements and Ultrasound Imaging, National-Regional Key Technology Engineering Laboratory for Medical Ultrasound, School of Biomedical Engineering, Shenzhen University Medical School, Shenzhen 518060, China.

[3]Institute of Biochemistry and Biophysics, Polish Academy of Sciences, Pawinskiego 5a, 02-106 Warsaw, Poland.

[4]School of Medicine, Southern University of Science and Technology, Shenzhen 518055, Guangdong, China.

[5]Department of Fundamental Microbiology, Faculty of Biology and Medicine, University of Lausanne, Biophore Building, CH-1015 Lausanne, Switzerland.

[6]Icahn School of Medicine at Mount Sinai, 1425 Madison Ave, New York city 10029, USA.

*Correspondence to Xue Liu: liuxuescience@gmail.com

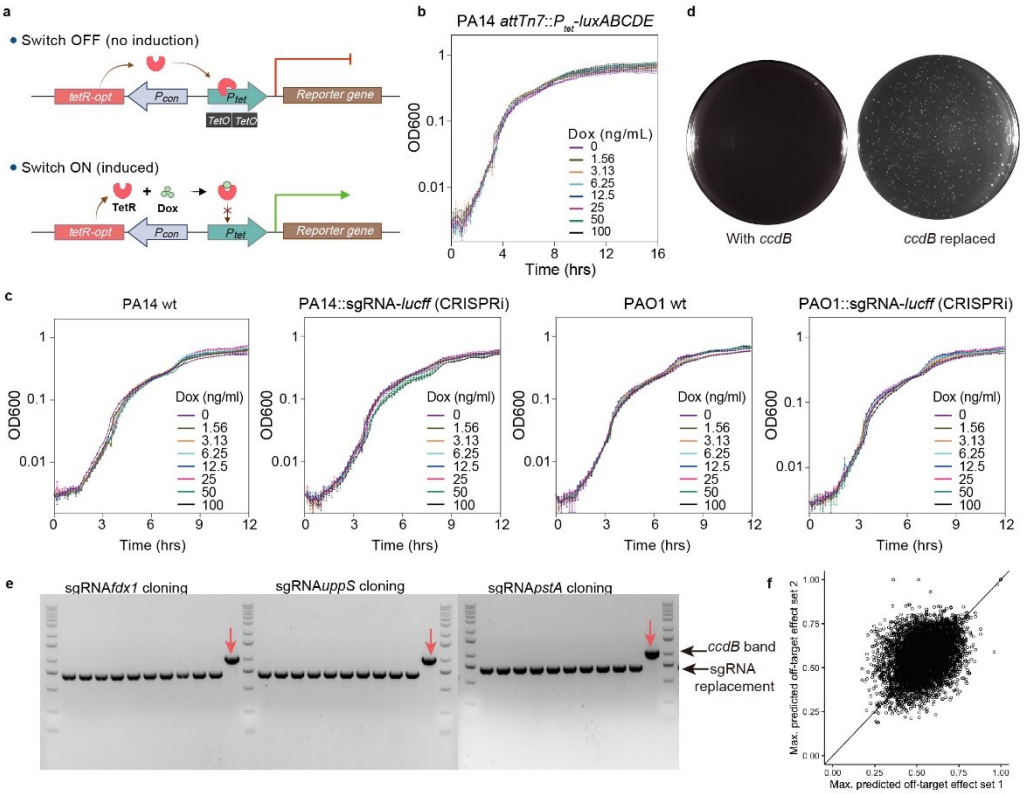

Supplementary Fig. 1. Evaluation of the tet-inducible CRISPRi system and CcdB-counter selection for sgRNA cloning. a. The designed tet-inducible system for *P. aeruginosa*. It includes a constitutive promoter (P_{con}) driving a codon-optimized TetR and a tet-inducible promoter (P_{tet}) initiating reporter gene expression. Dox presence inhibits TetR binding to *tetO* on P_{tet}, enabling reporter gene transcription. **b.** Growth of *P. aeruginosa* PA14 carrying the tet-inducible system in LB medium supplemented with increasing concentrations of Dox. **c.** Growth of *P. aeruginosa* with or without CRISPRi system in LB medium with various concentrations of Dox. PAO1 and PA14 strains were engineered with a CRISPRi system expressing dCas9 and an sgRNA targeting the luciferase reporter gene *lucff*. As *lucff* is absent from the native genomes of PAO1 and PA14, this setup enables assessment of potential growth defects solely attributable to dCas9 expression. **d, e.** Evaluation of background and efficiency of sgRNA cloning based on *ccdB* replacement. **f.** The off-targeting score of sgRNAs in the two sets of libraries. Source data are provided as a Source Data file.

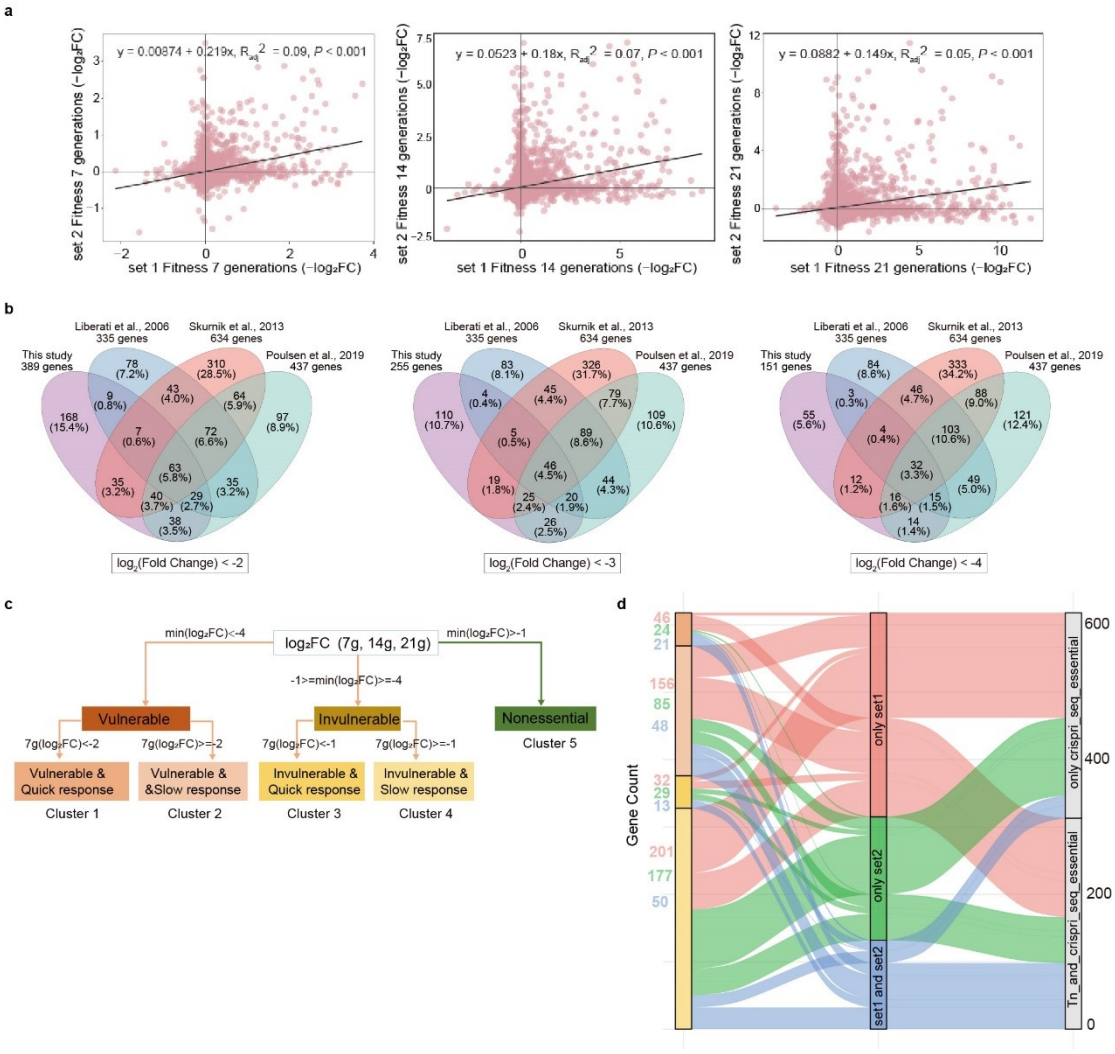

Supplementary Fig. 2. Assessment of the gene essentiality in *P. aeruginosa* via CRISPRi-seq. a. Correlation of gene fitness evaluated by set 1 and set 2 libraries, across 7, 14 and 21 generations of Dox induction. **b.** Comparative analysis of candidate essential genes from CRISPRi-seq, evaluated at different cutoffs of log_2FC (-2, -3 or -4) and comparison with Tn-seq screens. **c.** The workflow for categorizing genes into five clusters based on response time and maximum log_2FC in PA14 utilizing CRISPRi-seq. **d.** Sankey plot illustrating the distribution of essential genes identified by CRISPRi-seq and their overlap with those defined in previous Tn-seq studies. Numbers in pink, green, and purple on the left represent genes uniquely identified by set 1 sgRNAs, set 2 sgRNAs, or by both sets, respectively. Source data are provided as a Source Data file.

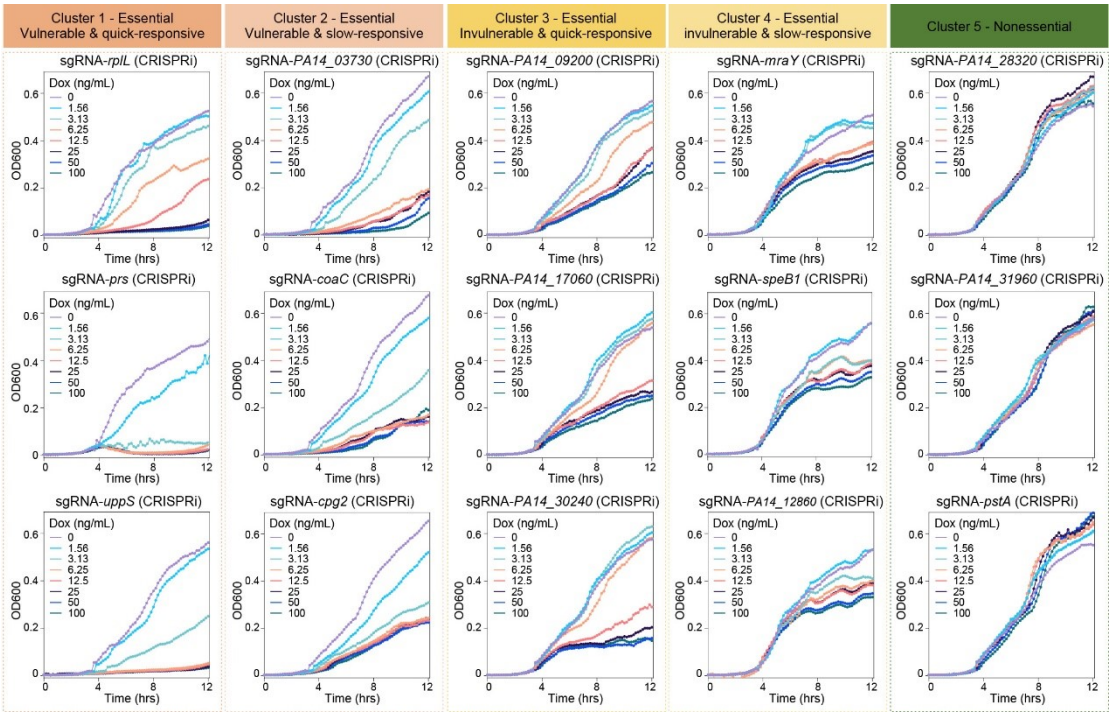

Supplementary Fig. 3. Growth of CRISPRi strains targeting representative genes from each of the 5 clusters defined in Supplementary Fig. 2c. Source data are provided as a Source Data file.

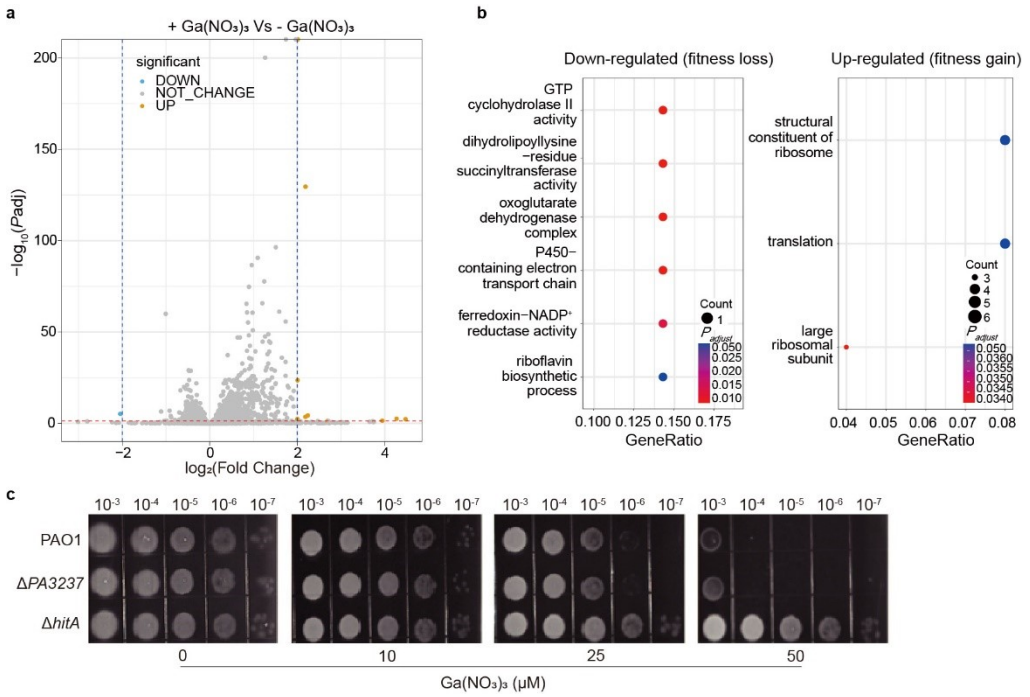

Supplementary Fig. 4. Impact of $Ga(NO_3)_3$ on *P. aeruginosa* growth. a. Volcano plots showing the CRISPRi-seq screening results with only 7-generations preinduction prior to $Ga(NO_3)_3$, which plotted gene fitness in log_2FC and -log_{10}(*P*adj value). Related to **Fig. 3c. b.** GO enrichment analysis of the genes with differential fitness in $Ga(NO_3)_3$-treated and untreated *P. aeruginosa,* identified by CRISPRi-seq. **c.** Deletion of *PA3237* (ortholog of *PA14_22320*) and *PA0287* (ortholog of *PA14_03760*) shows no growth difference under gallium treatment compared to wild-type PAO1. In contrast, deletion of *hitA* increases PAO1 resistance to gallium. Source data are provided as a Source Data file.

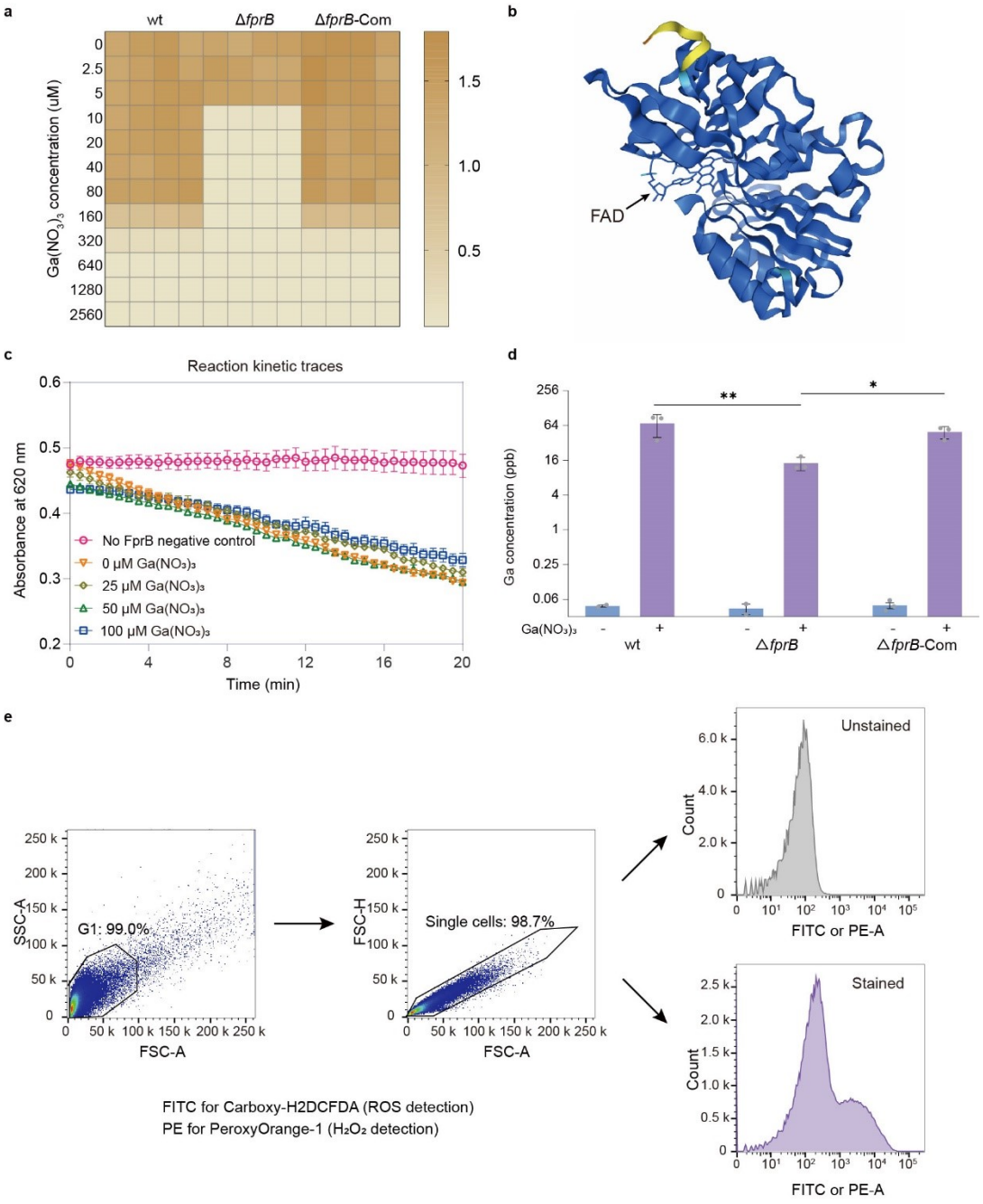

Supplementary Fig. 5. Functional analysis of FprB. a. MIC determination of $Ga(NO_3)_3$ for *P. aeruginosa.* Bacteria were cultured in 96-well plates for 24 hours at 37°C with 4 replicates in one plate per strain. **b.** AlphaFold3 predicted FprB to bind FAD. **c.** Dose-response curves for the FprB 2,6-dichlorophenolindophenol (DCPIP)-diaphorase activity in the absence or presence of $Ga(NO_3)_3$. Negative control contains all reactants but no FprB. **d.** Intracellular gallium concentration of *P. aeruginosa* under $Ga(NO_3)_3$ treatment. Data are presented as mean ± SD. The asterisks represent a significant difference from indicated groups with $^{**}P < 0.01$, $^{***}P < 0.001$ and $^{****}P < 0.0001$ by two-way ANOVA and Tukey's multiple-comparison test. **e**. Gating strategy for flow cytometric analysis of ROS and H_2O_2 levels (related to **Fig. 5b**). Flow cytometry acquisition captured 100,000 ungated events per sample using standardized parameters. Single live cells were gated (G1) using FSC-A/SSC-A parameters, followed by FSC-H/FSC-A doublet exclusion. Fluorescence thresholds were defined as fluorescence intensity exceeding 2-fold over unstained controls, with background signal quantified from non-stained parallel samples. Source data are provided as a Source Data file.

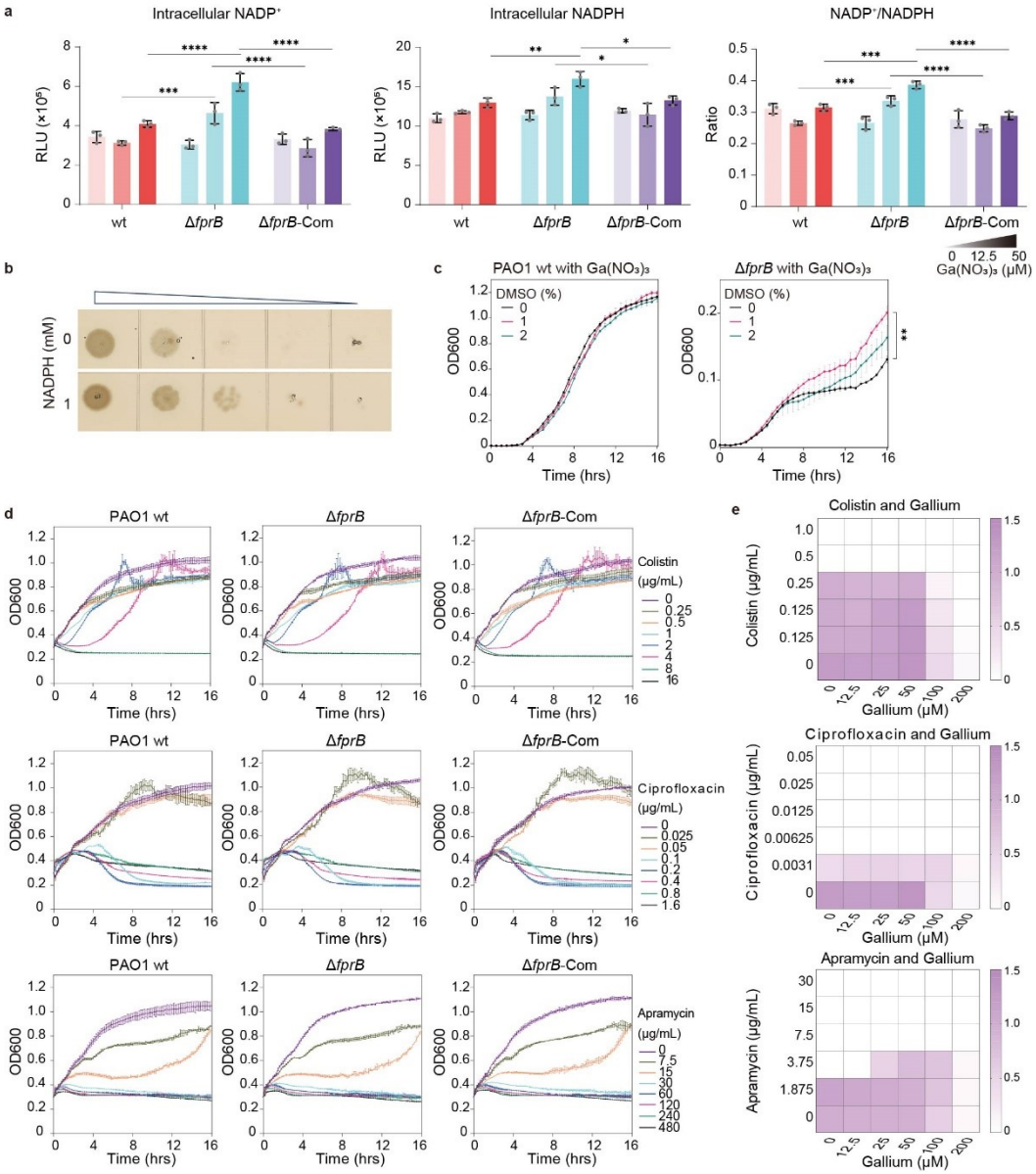

Supplementary Fig. 6. Influence of redox modulation and ROS-related interventions on gallium sensitivity in the Δ*fprB* mutant. a. Intracellular $NADP^+$ and NADPH accumulation. Bacteria (initial OD600 of 0.01) were cultured for 4 hours in LB broth with or without $Ga(NO_3)_3$. Luminescence value measured by a microplate reader were normalized to final OD600. Data are presented as mean ± SD. The asterisks represent a significant difference from indicated groups with $^*P < 0.05$, $^{**}P < 0.01$, $^{***}P < 0.001$ and $^{****}P < 0.0001$by two-way ANOVA and Tukey's multiple-comparison test. **b.** Plate spot assay of the Δ fprB strain comparing growth in the presence of 6.25 μM $Ga(NO_3)_3$ with or without 1 mM NADPH. Bacterial cultures were adjusted to an initial OD_{600} of 0.003 to assess the impact of NADPH supplementation on $Ga(NO_3)_3$-induced growth inhibition. **c.** DMSO supplementation partially rescued the growth defect of the Δ*fprB* mutant exposed to $Ga(NO_3)_3$ and NADPH. Bacterial cultures were adjusted to an initial OD600 of 0.003. Assays were conducted with 6.25 μM $Ga(NO_3)_3$. **d.** Assessment of FprB as a synergistic target for ROS-inducing antibiotics. Bacteria with an initial OD600 of 0.3 were cultured with or without the antibiotics colistin, ciprofloxacin or apramycin. **e.** Checkerboard assays evaluating potential synergistic interactions between gallium and the antibiotics colistin, ciprofloxacin, or apramycin. Source data are provided as a Source Data file.

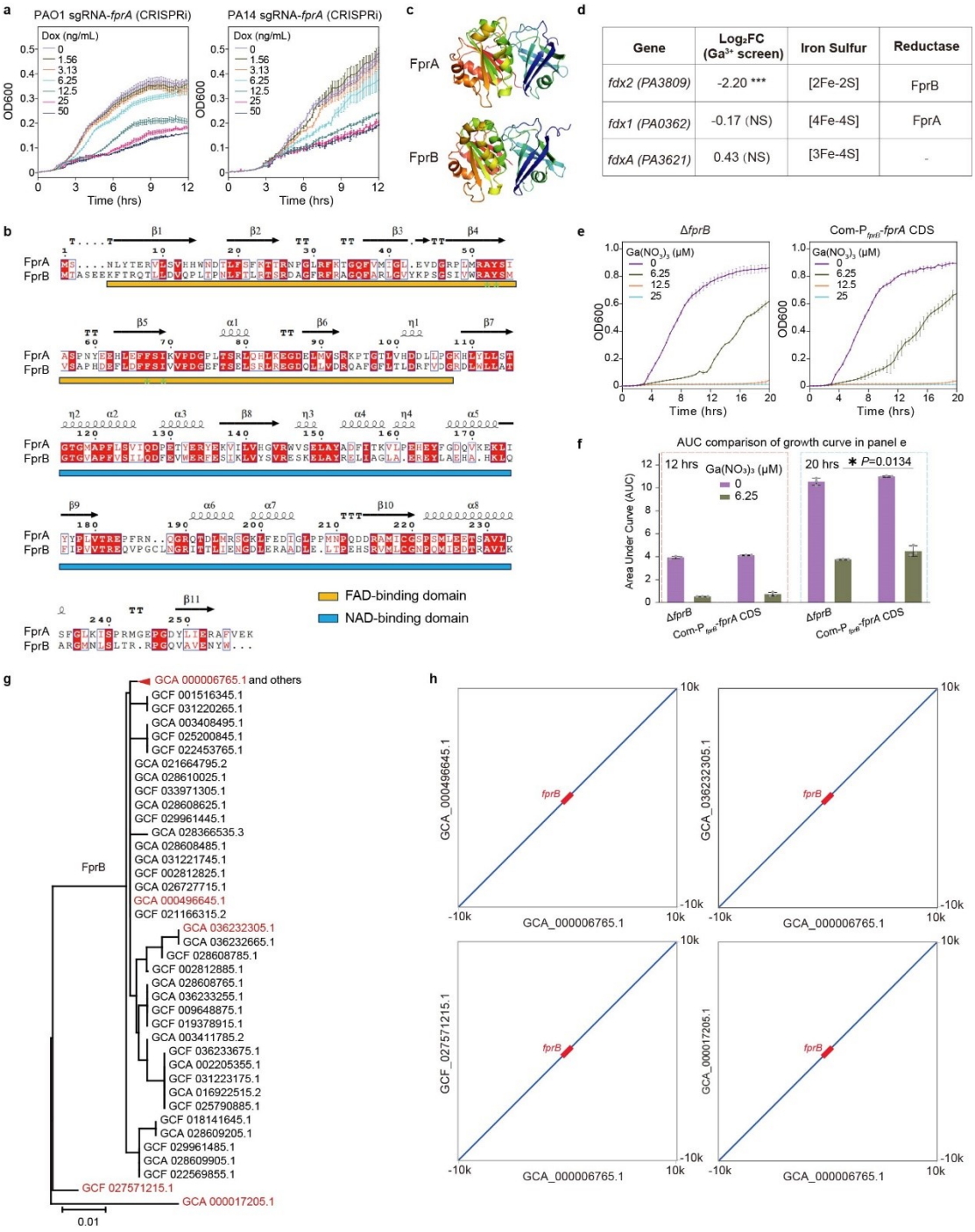

Supplementary Fig. 7. Evolutionary conservation and functional distinction of FprB from FprA revealed by genetic, phylogenetic, and comparative analyses. a. CRISPRi-mediated knockdown of *fprA* resulted in growth defects in both PAO1 and PA14 strains. **b, c**. Sequence alignment showing FprA exhibits approximately 42% amino acid sequence identity with FprB in *P. aeruginosa*. **d.** CRISPRi-seq screen under $Ga(NO_3)_3$ stress did not identify FprA and its substrate Fdx1 as contributors to gallium resistance. **e, f.** Complementation of *fprA* under the *fprB* promoter in the Δ*fprB* mutant led to a slight increase in gallium tolerance at 20 hours (P = 0.0134), with limited biological impact. Comparison of area under the curve (AUC) between gallium-treated and untreated bacteria for 12 and 20 hours, analyzed by two-way ANOVA and Tukey's multiple-comparison test. Data are presented as mean ± SD. Asterisks indicate significant differences (*$P < 0.05$) from the indicated groups. **g.** Neighbor-Joining phylogenetic tree of FprB proteins in representative *P. aeruginosa* strains. In total, 71 phylogenetic sub-clusters were detected from the 981

surveyed *P. aeruginosa* strains. The FprB proteins were collected from the representative strains of each sub-cluster, and used for phylogenetic tree building. The strains for which the genome accessions highlighted in red were used for further comparative genomic analysis. **h.** Collinearity analysis between *P. aeruginosa* strains representing different FprB sequence clusters for the *fprB* loci (indicated) and their 10k flanking sequences. Source data are provided as a Source Data file.